biomedical terms were often used instead of the traditional Kampo terms to avoid confusion.

Organ system patterns are very important in medicine in China and Korea. However, Kampo experts in the Meiji (1868–1912), Taisho (1912–1925), and Showa (1926–1989) eras chose not to use organ systems to avoid overlap with biomedical terms. As a result, Kampo medicine is sometimes criticized because of the relative lack of terms to describe patients' conditions. The pathogenesis rather than host reaction is most important in Western biomedicine. In contrast, the host's reaction to the pathogen is the most important factor in traditional medicine. In this regard, Kampo medicine has been developed in harmony with Western biomedicine.

5. Kampo Medicine Patterns

Kampo patterns were reconstructed logically according to the ICD principles, which are both jointly exhaustive and mutually exclusive. Several parameters are used for determining Kampo patterns: yin-yang, deficiency-excess, cold-heat, 6 stages of acute febrile diseases, and qi-blood-fluid [18]. Of these, yin-yang, deficiency-excess, cold-heat, and interior-exterior belong to the 8 principles used in Chinese medicine. In China, each component is used in combination with the others to define the pattern, such as "liver yin deficiency pattern," and is not usually used independently. Among 8 principles, yin-yang is a polysemic word. Sometimes it is used for the sensible temperature in Japan. Under international harmonization, yin-yang is usually a high-level concept of deficiency-excess, cold-heat, and interior-exterior. To avoid confusion, we decided not to use yin-yang for the sensible temperature.

Kampo patterns are determined for all patients according to the flow charts shown in Table 1 and Figure 1. Patient conditions are divided into 2 groups: acute febrile infectious conditions and chronic conditions (Figure 1). A 6-stage pattern, based on Shang Han Lun, is used for describing acute febrile infectious diseases like influenza. Qi-blood-fluid patterns are mainly used for describing chronic diseases.

One issue raised regarding Kampo patterns concerns the "between deficiency and excess" pattern. The deficiency and excess pattern is usually based on the strength of the pathogen. However, in Japan, deficiency and excess patterns are primarily based on the patient's condition. The ancient textbook of Huangdi Neijing (Former Han dynasty; 220 AD to 8 AD) explains that "when the foreign pathogen is strong, it is called as excess, and when body energy is weakened, it is called as deficiency." The problem with this statement is that deficiency is defined by the strength of foreign pathogens, and deficiency is defined by the energy of the host. Many traditional medical terms are polysemic, mainly due to their long history. However, the deficiency-excess terms are originally polysemic; this has created much confusion.

In Japan, deficiency-excess was originally determined by the strength of the foreign pathogen in the case of acute febrile infectious diseases and by the strength of the body energy in the case of chronic diseases. Additionally, Kampo medicine

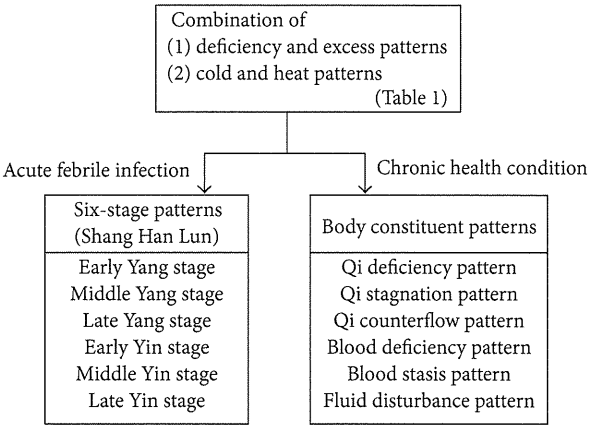

FIGURE 1: Diagnostic flow used in Kampo medicine. All patients are assigned a specific category as described in Table 1 and then divided into 2 groups according to whether they have acute febrile infectious disease or chronic disease. For acute febrile disease, the 6 stages of Shang Han Lun are very important. For chronic diseases, the host body constituent patterns are very important.

was used extensively for acute febrile infectious diseases before antibiotics were developed, where the strength of the foreign pathogen was very important. Since the development of antibiotics, Kampo medicine has been used more often for chronic diseases, in which the strength of the body energy is more important. In the modern version of Kampo, the host condition is assigned a high value, while the foreign pathogen is addressed by Western biomedicine. Therefore, the host energy is of greater importance. The need thus arose for the option to designate the body energy level as "neutral" rather than just "deficient" or "excessive." This issue was raised by Tokaku Wada (1743–1803), a physician in the Edo period [19]. His clinical wisdom was described in "Dosui Sagen" which was published in 1805. In this book, "between deficiency and excess" was described in the type of edema. This idea is thought to have influenced Kazuo Tatsuno (1905–1976) [20, 21] and other physicians in the Showa era. For example, a patient with impaired glucose tolerance appears normal according to the older Kampo designations, even though Kampo medicine is indicated for this condition. In such cases, the "neutral" designation enables acknowledgment of a condition that lies between deficiency and excess.

6. Formula Pattern

The formula pattern is also very unique in Kampo medicine. While traditional Chinese medicine (TCM) prescriptions are individualized at the herbal level, Kampo medicine is individualized at the formula level. This practice may have started during the Edo period, as usage of different amounts of herbs was described in a book by Kaibara in 1712 [22]. According to this book, the amount of each herb used in Japan was 1/5 to 1/3 that used in China. Kaibara explained that one of the reasons for this practice was the difficulty in importing herbs from China. Even though alternative herbs available in Japan were used, some had to be imported from

Table 1: Combinations of deficiency-excess and cold-heat patterns.

Components	Cold	Heat	Between cold and heat	Tangled cold and heat
Deficiency	Cold, deficiency	Heat, deficiency	Between cold and heat, deficiency	Tangled cold and heat, deficiency
Excess	Cold, excess	Heat, excess	Between cold and heat, excess	Tangled cold and heat, excess
Between deficiency and excess	Cold, between deficiency and excess	Heat, between deficiency and excess	Between cold and heat, between deficiency and excess	Tangled cold and heat, between deficiency and excess

Regardless of acute or chronic health conditions, all patients are classified into 1 of these 12 combinations. Very limited combinations are used for acute diseases. Between deficiency and excess; neutral in "deficiency and excess"; between cold and heat; neutral in "cold and heat"; tangled cold and heat; mixture "cold and heat," for example, cold foot and hot flush on face.

China. These differences in the amounts of herbs used are still prevalent. This may explain why Kampo medicine is individualized at the formula level. During the Edo period, doctors carefully studied the roles of formulas and decided the characteristics of each formula. This practice led to Yoshimasu's idea of "matching of pattern and formula."

Physicians continue to follow this principle today. Clinical trials have been conducted using the same Kampo formula used previously for a specific disease, determining the appropriate Kampo formula based on host patterns. "Matching of pattern and formula" has thus been shown to be a sophisticated approach.

By 1967, the first 4 Kampo formulas were approved by the government for coverage under the national insurance system, and 148 are now listed.

The acceptance of Kampo formulas into the national health insurance system marked the start of the exponential growth of Japan's market in Kampo medicines. Between 1976 and 1992, the sales of Kampo medicine grew more than 10-fold in Japan (Japan Kampo Medicine Manufacturers Association, 2007) [23].

With such a rapid increase in the number of Kampo drug products sold, the government and pharmaceutical industry needed to ensure that high standards were maintained. In 1987, the government established the Good Manufacturing Practice (GMP) law to ensure safety in manufacturing processes, including the production of Kampo formulas. The stringent manufacturing process for Kampo medicine has increased the legitimacy of this modality, as people can now expect uniformity and high quality from the different formulas. This facilitates "matching of pattern and formula," because if the formulas are not stable, it is very difficult to consistently match pattern to formula.

7. Future Challenges

Even though all 80 medical schools in Japan have incorporated Kampo medical courses into their curricula, the number of such courses is very small compared to that of Western biomedicine courses. Postgraduate and continuous Kampo medical education have not been established. Statistics indicate that Kampo formulas are used in daily practice by 90% of physicians, which represents over 260,000 physicians. However, the number of Kampo experts certified by the JSOM is only 2150. This great discrepancy means that most physicians use Kampo formulas based on Western biomedical disease diagnoses without deep consideration of patterns. Further education is necessary for the users of Kampo formulas.

Another concern for the future is the coding rule used for the qi-blood-fluid pattern. Deficiency, excess, and between deficiency and excess are mutually exclusive. Likewise, cold-heat and the 6 stages are mutually exclusive in the same category. However, several abnormalities in qi-blood-fluid may exist in 1 patient. We conducted a small clinical trial without establishing any coding rules. Some doctors provided only 1 code for the qi-blood-fluid pattern, while others provided 4 codes. For more accurate statistics, coding rules should be developed and training in coding should be imparted.

In terms of international comparisons, Kampo patterns are too simple compared to TCM and traditional Korean medicine (TKM). Organ system patterns are particularly lacking in Japan. However, in ICD-11, all the patterns will be presented on the common platform of Western biomedicine. Some organ system patterns can be linked to Western biomedicine disease codes, even though they do not map one-to-one. ICD 11 has terminology that is novel to ICD. This allows ontology software precisely describe the content of each term and links the different codes to each other. The next stage of ICTM development will be field testing. We expect that the international field test will allow for international comparisons.

8. Conclusion

Kampo patterns are rather unique compared to Chinese or Korean patterns. There are 2 explanations for this difference. First, Kampo medicine was separated from the theory of the Ming dynasty and then reestablished based on Shang Han Lun theory during the Edo period. Second, Kampo medicine is used in combination with Western biomedicine by licensed doctors in Japan. Kampo terminology was redeveloped in order to avoid confusion with Western biomedicine.

Conflict of Interests

The authors declare that there is no conflict of interests regarding the publication of this paper.

Acknowledgment

This work was supported by a Grant-in-Aid for Research on Applied Use of Statistics and Information, Health and Labour Sciences Research and Clinical Research for Development of Preventive Medicine and New Therapeutics from the Ministry of Health, Labour and Welfare.

References

[1] WHO Medicines, "Traditional and Complementary Medicine," http://www.who.int/medicines/areas/traditional/en/.

[2] Declaration of Alma-Ata International Conference on Primary Health Care, Alma-Ata, USSR, September 1978, http://www.who.int/publications/almaata_declaration_en.pdf.

[3] P.-F. Gao and K. Watanabe, "Introduction of the World Health Organization project of the International Classification of Traditional Medicine," *Journal of Chinese Integrative Medicine*, vol. 9, no. 11, pp. 1161–1164, 2011.

[4] K. Watanabe, X. Zhang, and S.-H. Choi, "Asian medicine: a way to compare data," *Nature*, vol. 482, no. 7384, p. 162, 2012.

[5] "ICD11 beta," http://apps.who.int/classifications/icd11/browse/f/en.

[6] G. S. de Morant, *Chinese Acupuncture*, Paradigm Publication, Tokyo, Japan, 1994.

[7] G. A. Plotnikoff, K. Watanabe, and F. Yashiro, "Kampo-from old wisdom comes new knowledge," *Herbal Gram*, vol. 78, pp. 46–57, 2008.

[8] K. Terasawa, "Evidence-based reconstruction of Kampo medicine: part I—is Kampo CAM?" *Evidence-Based Complementary and Alternative Medicine*, vol. 1, no. 1, pp. 11–16, 2004.

[9] K. Watanabe, K. Matsuura, P. Gao et al., "Traditional Japanese Kampo medicine: clinical research between modernity and traditional medicine—the state of research and methodological suggestions for the future," *Evidence-Based Complementary and Alternative Medicine*, vol. 2011, Article ID 513842, 19 pages, 2011.

[10] E. C. Moschik, C. Mercado, T. Yoshino, K. Matsuura, and K. Watanabe, "Usage and attitudes of physicians in Japan concerning traditional Japanese medicine (Kampo medicine): a descriptive evaluation of a representative questionnaire-based survey," *Evidence-based Complementary and Alternative Medicine*, vol. 2012, Article ID 139818, 13 pages, 2012.

[11] A. Ito, K. Munakata, Y. Imazu, and K. Watanabe, "First nationwide attitude survey of Japanese physicians on the use of traditional Japanese medicine (Kampo) in cancer treatment," *Evidence-Based Complementary and Alternative Medicine*, vol. 2012, Article ID 957082, 8 pages, 2012.

[12] G. A. Plotnikoff and K. Watanabe, "New insights on women's health from Japan," *Minnesota Physician*, vol. 12, pp. 32–33, 2004.

[13] V. Scheid, T. Ward, W.-S. Cha, K. Watanabe, and X. Liao, "The treatment of menopausal symptoms by traditional East Asian medicines: review and perspectives," *Maturitas*, vol. 66, no. 2, pp. 111–130, 2010.

[14] Y. Gepshtein, G. A. Plotnikoff, and K. Watanabe, "Kampo in women's health: Japan's traditional approach to premenstrual symptoms," *Journal of Alternative and Complementary Medicine*, vol. 14, no. 4, pp. 427–435, 2008.

[15] Y. Sahashi, "Herbs covered by health insurance in Japan," *The Journal of Kampo, Acupuncuture and Integrative Medicine*, vol. 1, pp. 70–84, 2005.

[16] F. Yu, T. Takahashi, J. Moriya et al., "Traditional Chinese medicine and kampo: a review from the distant past for the future," *Journal of International Medical Research*, vol. 34, no. 3, pp. 231–239, 2006.

[17] S. Cameron, H. Reissenweber, and K. Watanabe, "Asian medicine: Japan's paradigm," *Nature*, vol. 482, no. 7383, p. 35, 2012.

[18] K. Terasawa, "Evidence-based reconstruction of Kampo medicine: part II— the concept of Sho," *Evidence-Based Complementary and Alternative Medicine*, vol. 1, no. 2, pp. 119–123, 2004.

[19] T. Wada, *Dosui Sagen*, K. Hayashi, Tokyo, Japan, 1805, (Japanese).

[20] K. Tatsuno, "Kyo-jitsu-ron (1)," *Journl of Kampo Medicine*, vol. 1, pp. 383–392, 1954 (Japanese).

[21] K. Tatsuno, "Kyo-jitsu-ron (2)," *Journl of Kampo Medicine*, vol. 1, pp. 445–457, 1954 (Japanese).

[22] E. Kaibara, *Yojokun*, Kodansha, Tokyo, Japan, 1982, Translated to modern Japanese by T. Ito.

[23] Japan Kampo Medicines Manufactures Association, http://www.nikkankyo.org/.

日本機械学会論文集（A編）
79巻802号（2013-6）

ノートNo. 2012-JAN-0997

空気噴流による柔軟物の粘弾性特性*

長尾 光雄[*1]，望月 康廣[*2]，西本 哲也[*1]，横田 理[*1]

Viscoelasticity of Soft Samples by Air Jet

Mitsuo NAGAO[*1], Yasuhiro MOCHIZUKI, Tetsuya NISHIMOTO and Osamu YOKOTA

[*1] Nihon Univ. College of Engineering, Dept. Mechanical Engineering
Tokusada, Tamura-machi, Koriyama-shi, Fukushima, 963-8642 Japan

There have been few reports on test methods for viscoelasticity properties of soft samples using an air jet instead of plungers for loading and unloading. Authors propose a method of evaluating their viscoelasticity properties, such as soft processed foods and industrial products, using the air jet with newly developed test equipment. In this method, loading and unloading can be performed using the air jet in a very short time, loading time can be arbitrarily set, and the shape of the dents formed on the surface of soft samples can be instantaneously measured using light from a semiconductor laser. Using the developed equipment, authors measured the shape of the dents formed on soft samples, measured the depth of the dents for various loading times, types of soft samples and pressures, and evaluated the viscoelasticity properties of the soft samples with respect to elastic compliance and equivalent dent depth.

Key Words : Viscoelasticity, Material Testing, Softness, Creep, Creep Recovery, Compliance, Nozzle, Laser-Aided Diagnostics, Laser Measurement

1. 緒　　言

柔軟物は，一定の外力が加えられるとクリープを起こし，除荷されるとクリープ回復を起こす．クリープ挙動やその回復挙動は，弾性変形を表わすばねと粘性を表わすダッシュポットの二つの要素を組み合わせた力学的モデルが利用され，弾性と粘性の係数が求められる．柔軟物の測定方法には，引張り，圧縮，ねじり，曲げ，およびひずみ変形などがあり，それらを測定する方法にはレオメータがある．これは，工業材料を対象にする万能試験機の機能を備えたもので，荷重と変形を同時に検出して柔軟物の破断や粘弾性を測定する．このときに用いられる圧子（プランジャー[(1)]あるいはアダプターを指す）には，針，コーン，円盤，球体，および板状刃などがあり，柔軟物や試験方法によって圧子を適切に選択して試験が行われる．例えば，ゲル状食品の試験には定荷重あるいは定速度で圧子を柔軟物に押し込む方法で粘弾性特性を調べる．しかし，圧縮，粘性，クリープ，および応力緩和などの試験により圧子が異なり，またその可動速度も柔軟物の急激な変形に対応しない場合がある．

本研究[(2),(3)]では，負荷および除荷を特定の圧子で行うのでなく，空気噴流を用いて柔軟物表面にくぼみを発生させ，その瞬時の形状変化をレーザ光により計測できる測定方法を提案し，その計測装置の開発を行っている．ここでは，柔軟物に与えた負荷時間や負荷の大きさによるくぼみ深さを測定し，そのクリープおよびクリープ回復挙動から，提案するコンプライアンスや等価深さによる柔軟物の粘弾性を評価したので報告する．

2. 柔軟物のクリープおよびクリープ回復挙動

図1はクリープおよびその回復曲線，図2はそのときの四要素等価モデルを示す．図1において，くぼみのクリープ挙動は時間 $t=0\sim t_r$ の間に空気噴流を柔軟物表面に負荷し続けたときのくぼみ深さの変化を示し，クリープ回復挙動は時間 $t=t_r$ で除荷したときのくぼみ深さの変化を示す．柔軟物表面に発生したクリープ挙動のくぼみ深さ $h_{(t)}$ は式（1）で表す．

* 原稿受付　2012年12月15日
*1 正員，日本大学工学部機械工学科（〒963-8642　福島県郡山市田村町徳定字中河原1番地）
*2 正員，日本大学大学院工学研究科博士後期課程
E-mail: nagao@mech.ce.nihon-u.ac.jp

$$h_{(t)} = h_1 + h_2 + h_3 = h_1' + h_2' + h_3' \tag{1}$$

式（1）のクリープ挙動は，図2に示したばねとダンパーを用いた式（2）[4]で示せる．

$$h_{(t)} = \frac{F}{G_1} + \frac{F}{G_2}\cdot\left\{1-\exp\left(-\frac{G_2}{\eta_2}\cdot t\right)\right\} + \frac{F}{\eta_3}\cdot t \tag{2}$$

式（2）において，第1項のG_1および第3項のη_3はマクスウェルモデルのばねの弾性率とダッシュポットの粘性率であり，第2項のG_2およびη_2はフォークトモデルのばねの弾性率とダッシュポットの粘性率である．柔軟物表面に生じるくぼみ深さのクリープ挙動において，くぼみ深さ$h_{(t)}$は荷重Fに依存するので次のように示せる．

$$h_{(t)} = J\cdot F \tag{3}$$

$$J = h_{(t)}/F \tag{4}$$

ここで，Jはくぼみ深さのコンプライアンスと呼ぶことにし，その単位はmm/Nで，1N当たりどの程度のくぼみ深さが得られたかを示す．式（4）は式（1）より次のように示せる．

$$J = h_1/F + h_2/F + h_3/F \tag{5}$$

一方，クリープ終了時，あるいはクリープ回復直前の最大くぼみ深さh_{tr}に対する任意の時間のくぼみ深さの割合をくぼみの等価深さと定義すると，式（1）は式（6）のように示せる．等価深さの単位は無次元である．

$$h_{(t)}/h_{tr} = h_1/h_{tr} + h_2/h_{tr} + h_3/h_{tr} \tag{6}$$

式（1），式（5），および式（6）の右辺の第1項，第2項，および第3項は，それぞれ最大くぼみ深さの変形に対する瞬間弾性変形，遅延弾性変形，および変形が残留する永久変形である．これらのことより，柔軟物の粘弾特性は，弾性率や粘性率でその物性を求める代わりにコンプライアンスや等価深さで表示することができる．

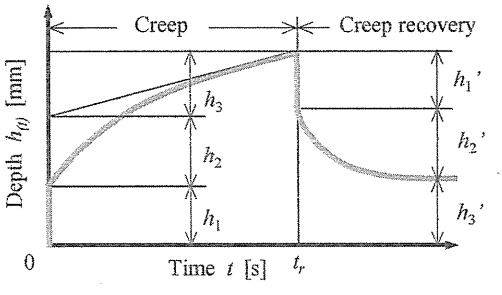

Fig.1　Viscoelasticity characteristics provided during creep and creep recovery processes.

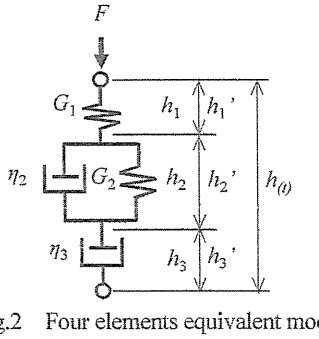

Fig.2　Four elements equivalent model.

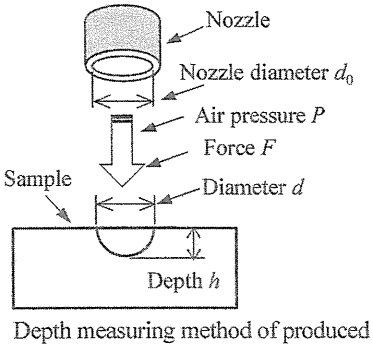

Fig.3　Depth measuring method of produced dents.

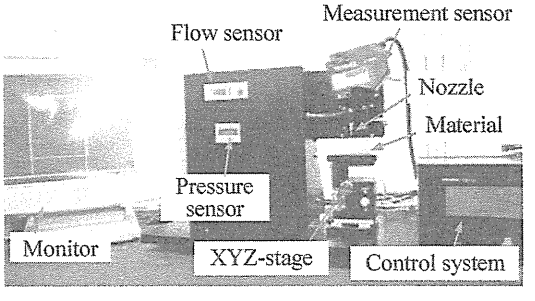

Fig.4　Summary of measuring equipment.

3. 柔軟物表面のくぼみの測定方法

本測定法は，空気噴流を利用する方法であるため，食品や生体部位[5]の柔らかさや粘弾性特性が測定できる計測装置である．図3に示すように，ノズルより噴き出した空気が柔軟物の表面に当たり，その表面にくぼみが生じる．くぼみは噴流の強さに大きく依存すると考え，噴流の強さによるくぼみ深さの時間的変化を測定することで，柔軟物の粘弾性特性が調べられる．計測装置の外観を図4に示した．なお，実験に用いたノズル口径 d_0=1.0mm，噴射距離5mmとし，柔軟物の寸法はくぼみ形状の測定に影響しない範囲の直径50mm，厚さ20mmにした．なお，対象とした柔軟物は，人肌ゲル，スライム，プリン，絹豆腐，および木綿豆腐である．

4. 実験結果

4・1 負荷時間を変化させた場合の粘弾性特性

図5はスライム表面に噴射圧力 P を20kPa一定として，噴射時間 t_r が5秒，10秒，15秒，および20秒の4段階に変えたときの負荷開始から100秒までのくぼみ深さのクリープおよびクリープ回復を示す．図5のくぼみ深さのクリープ曲線は，非線形を示す遅延弾性変形と永久変形が表れる．負荷時間が短いとくぼみは浅く，負荷時間が長くなると，その深さは深くなる．また，クリープ曲線は負荷時間に関わらず，一つの曲線で示された．クリープ回復曲線の瞬間弾性変形はわずかに現われるが，遅延弾性変形は長い時間を必要としており，永久変形も残留する．

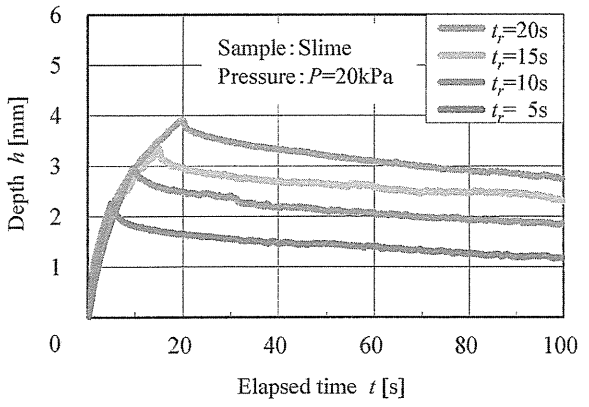

Fig.5 Variation of dents depth for creep time.

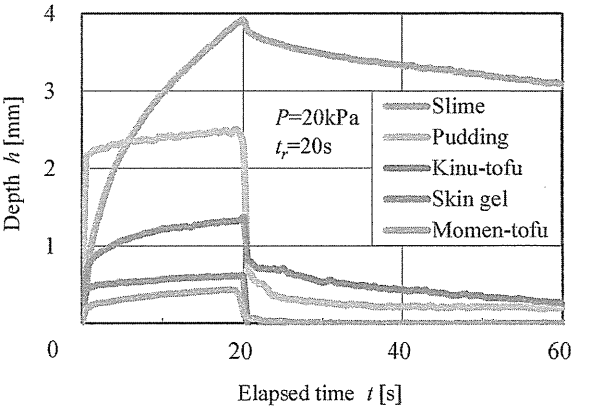

Fig.6 Variation of dents depth which appeared on soft samples.

4・2 各種柔軟物による粘弾性特性

図6には，スライムと人肌ゲルの工業材料，プリン，絹豆腐，および木綿豆腐の加工食品のくぼみ深さのクリープおよびクリープ回復挙動を示した．このときの負荷条件は，それぞれ噴射圧力20kPa，噴射時間20秒，経過時間60秒とした．負荷時間7秒までのくぼみ深さは，プリンが最も大きいので柔らかく，続いてスライム，絹豆腐，人肌ゲル，木綿豆腐の順に小さくなる．しかし，7秒を過ぎると，スライムとプリンのくぼみ深さは逆転し，スライムの方が深くくぼむ．これらの挙動については，プリンは瞬間弾性変形の占める割合が大きく，遅延弾性変形や永久変形の占める割合が少ないためであり，スライムは永久変形の占める割合が大きく，瞬間弾性変形や遅延弾性変形は少ない．負荷停止後の40秒間におけるくぼみ深さのクリープ回復は，スライムはゆっくり回復し，続いて絹豆腐，プリン，木綿豆腐，人肌ゲルの順にくぼみ深さが浅くなる．スライムは瞬間弾性変形がほとんどなく，遅延弾性変形の占める割合が大きいと考える．一方，プリンと絹豆腐は，瞬間弾性変形，遅延弾性変形，および永久変形の3つの挙動が現われるが，人肌ゲルと木綿豆腐の場合はクリープ回復の大部分は瞬間弾性変形である．

4・3 圧力を変化させた場合の粘弾性特性

図7は，人肌ゲルと絹豆腐に対して圧力変化を5段階に分け，負荷時間20秒とし，除荷後の時間軸に対するくぼみ深さの変化について示した．負荷圧力は，人肌ゲルは40kPa～60kPaの範囲，絹豆腐は20kPa～40kPaの範囲

で5kPaごとにくぼみの深さを測定した．(a) の人肌ゲルは，負荷直後のくぼみの発生は瞬間に現われ，また除荷直後も瞬間にくぼみ深さが回復し，その後，5秒以内で完全に回復している．人肌ゲルは瞬間弾性変形が強い柔軟物であることが分かる．(b) の絹豆腐のクリープは図6から分かるように，人肌ゲルとスライムの中間の挙動を示す．負荷直後では瞬間弾性変形を示し，その後粘弾性挙動を示す．除荷直後には瞬間弾性変形を示した後，緩やかに遅延弾性変形の回復を示し，80秒後には負荷圧力に相応した永久変形が見られる．くぼみ深さ曲線には，凸凹の小さな振幅が現われている．これは，豆腐製造工程における気孔の発生，水の量および食物繊維や凝固剤の分量が影響したものと考える．

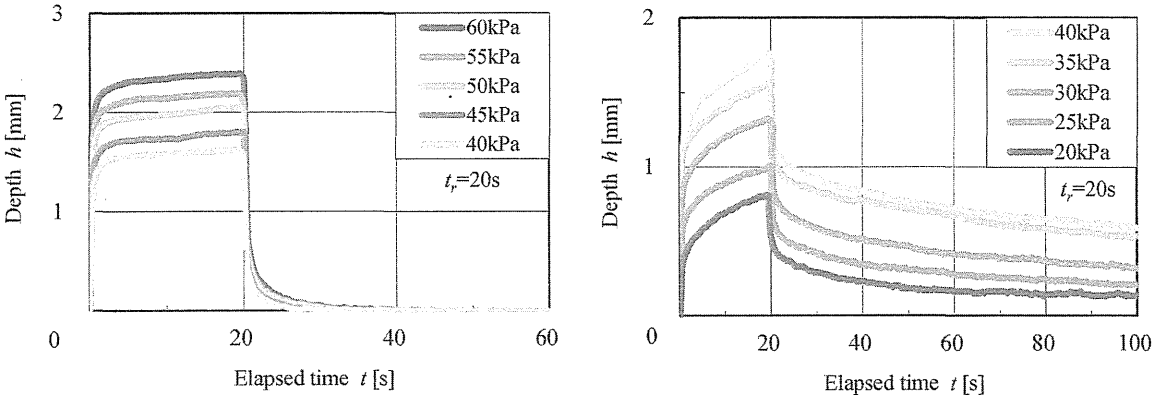

(a) Skin gel　(b) Kinu-tofu

Fig.7　Elapsed time of dents depth on soft samples for pressure.

5. 考　　察

5・1　クリープおよびクリープ回復のコンプライアンス

図7に示した人肌ゲルおよび絹豆腐について，式 (5) より算出したそれぞれの挙動に対するコンプライアンスの経過時間を図8に示す．図8 (a) の人肌ゲルにおいては，各圧力で得られたクリープ挙動のコンプライアンスおよびクリープ回復挙動のコンプライアンスはほぼ一つの合成曲線で示された．しかし，(b) の絹豆腐の場合には，両曲線にばらつきのある曲線になっている．これらの理由として，人肌ゲルとスライムなどの工業製品は，製造方法，組成や機械的特性の規格が統一されているため，本測定結果はほぼ同じ結果になったと予想される．一方，豆腐やかまぼこなどの加工食品は，気孔の存在があり，弾力性，歯切れ度，および硬さなどが統一されていないことが原因と考える．表1は，噴射圧力40kPaを負荷したときの人肌ゲルと絹豆腐の最大くぼみ深さ h_{tr} におけるクリープ挙動のコンプライアンスを式 (5) より算出した結果である．人肌ゲルのそれは，h_1/F=68 mm/Nで最も大きく，続いて h_2/F=12 mm/N，h_3/F=5 mm/N となった．絹豆腐では，h_1/F=60 mm/N が大きく，続いて h_3/F=22 mm/N，h_2/F=10 mm/N の順になった．したがって，これらには瞬間弾性変形，遅延弾性変形，および永久変形が異なる機械的特性を有していることが分かる．

5・2　クリープおよびクリープ回復のくぼみの等価深さ

図7に示した人肌ゲルと絹豆腐ついて，式 (6) より算出したそれぞれの挙動に対する等価深さを調べ，得られた結果を図9に示す．図9 (a) の人肌ゲルの等価深さ曲線はコンプライアンス曲線と同様に一つの合成曲線で示され，(b) の絹豆腐の等価深さ曲線はばらつきのある曲線になっている．表2には，噴射圧力40kPaを負荷した人肌ゲルと絹豆腐の最大くぼみ深さ h_{tr} におけるクリープ挙動の等価深さを示す．人肌ゲルの等価深さは，h_1/h_{tr}=80 %と高い割合を占め，続いて h_2/h_{tr}=14 %，h_3/h_{tr}=6 %の割合になった．絹豆腐では，h_1/h_{tr}=65 %，続いて h_3/h_{tr}=24 %，h_2/h_{tr}=11 %になった．したがって，これらは，瞬間弾性変形，遅延弾性変形，および永久変形の占める割合が分かる．

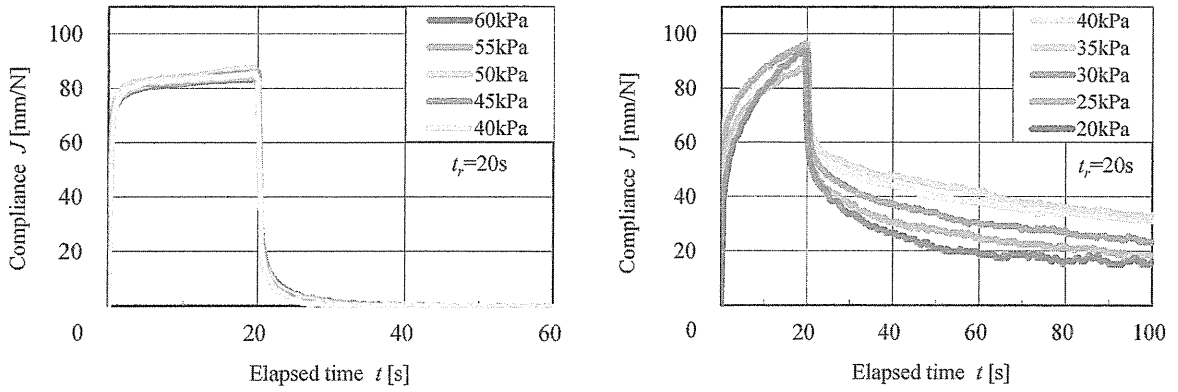

(a) Skin gel (b) Kinu-tofu

Fig.8 Elapsed time and compliance for pressure.

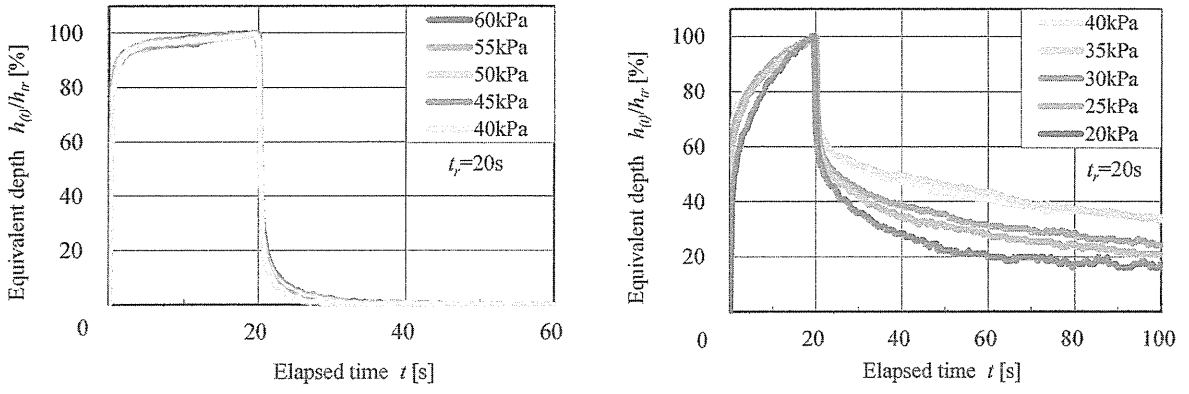

(a) Skin gel (b) Kinu-tofu

Fig.9 Elapsed time and equivalent depth for pressure.

Table 1 Creep compliance for pressure at 40 kPa.

	h_1/F [mm/N]	h_2/F [mm/N]	h_3/F [mm/N]
Skin gel	68	12	5
Kinu-tofu	60	10	22

Table2 Creep equivalent depth for pressure at 40 kPa.

	h_1/h_{tr} [%]	h_2/h_{tr} [%]	h_3/h_{tr} [%]
Skin gel	80	14	6
Kinu-tofu	65	11	24

6. 結　　言

空気噴流による柔軟物のくぼみ深さの測定法を提案し，その粘弾性特性を調べた．得られた結果を要約する．

(1) 空気噴流を柔軟物表面に瞬時に負荷・除荷させ，くぼみ深さの粘弾性特性が調べられる．

(2) 柔軟物による瞬間弾性変形，遅延粘弾性変形，および永久変形の特性が確認できた．

(3) クリープとクリープ回復の測定が簡単にでき，またくぼみ深さのクリープ挙動に関わるコンプライアンスや等価深さが評価できた．

文　　献

(1) 仲濱信子，大越ひろ，森高初恵，“おいしさのレオロジー”，(2012)，pp.56-67，アイ・ケイ コーポレーション．

(2) 横田 理，“柔らかさ測定方法及び柔らかさ測定装置”，特許 4247474,(2009),平成 21 年．

(3) 長尾光雄，横田 理，依田満夫，“柔らかさおよび粘弾性を計測できる機能性試験機の開発”，日本機械学会論文集 C 編, Vol.76, No.770 (2010), pp.2598-2603.

(4) 後藤兼平，平井西夫，花井哲也，レオロジーとその応用，(1962)，pp.74-88，共立出版．

(5) 西本哲也，永井孝太，“自動車急制動時の下肢筋電応答に及ぼす加齢の影響”，日本機械学会論文集 C 編，Vol.78, No.792 (2012), pp.2962-2971.

Journal of Mechanics Engineering and Automation 3 (2013) 405-413

Development of a Finger-Shaped Muscle Hardness Tester and Its Measurement Cases

Mitsuo Nagao[1], Kotaro Yatabe[2], Shin-ichi Konno[3], Tokuo Endo[4] and Osamu Yokota[1]

1. College of Engineering, Nihon University, Koriyama 963-8642, Japan

2. Graduate School of Engineering, Nihon University, Koriyama 963-8642, Japan

3. Department of Orthopedic Surgery, Fukushima Medical University, Fukushima 960-1295, Japan

4. Endo-Osteopathic Clinic, Motomiya 969-1129, Japan

Received: May 2, 2013 / Accepted: June 6, 2013 / Published: July 25, 2013.

Abstract: As the background of our study, we requested that practitioners use muscle hardness testers to conduct a digital assessment of muscle hardness layers that they can feel by palpation. We developed muscle hardness testers to assess muscle hardness digitally from the reaction force and the depth in pushing a finger-shaped indenter, thereby simulating palpation. To assess muscle hardness digitally, we proposed this means using the reaction force and depth that are measured when the indenter is pushed, along with the elastic constant, and the differential elastic modulus. The tester is designed to be useful to ascertain effects of, or follow the course of, muscle layer treatment applied for shoulder stiffness and other conditions. As described herein, we confirmed the effectiveness of digital assessment using foam rubber consisting of an upper layer and a lower layer, respectively simulating the cortical and muscle layers of a human body. Additionally, monitoring six subjects, we digitally assessed the change of hardness of the trapezius muscle by changing the position of the upper extremity. Next, we were able to measure the change of hardness before and after treatment for 21 subjects with shoulder stiffness.

Key words: Muscle hardness tester, finger-shaped, trapezius muscle, shoulder stiffness, palpation.

1. Introduction

The objective of this study is the development of a muscle-hardness measuring device [1] that converts muscle hardness into digital signals after sensing by pressing a finger-shaped indenter, simulating palpation. The muscle hardness detection methods used by commercially available devices and those described in the literature are of five categories, respectively assessing displacement [2-5], inclination angle [6-7], viscoelasticity [8-10], mechanical impedance [11-12], and impulse [13]. These devices have their respective benefits and shortcomings, but none has been completely accepted by practitioners who must diagnose patients [4-5, 10, 14-17]. This fact is attributable to a lack of knowledge about the fatty layer thickness and differences of its flexibility. Furthermore, the reliability of measurements and operability need improvement.

The authors are striving to realize a digital assessment method that is insensitive to these conditions and to develop a measuring device that can accommodate small changes in hardness, hardness of deep muscle layers, enhanced effects of treatment, and which allows follow-up monitoring. In other words, muscle layer hardness caused by shoulder stiffness, lumbago, and fatigue can be digitalized.

This paper presents an outline of the proposed measuring device, its method of digitalization, and its effectiveness and validity as confirmed through experiments. First, digitalization of hardness of the lower layer of foam rubber consisting of the upper/lower two layers are checked. Second, changes

Corresponding author: Mitsuo Nagao, associate professor, Ph.D., research fields: measurement and diagnosis systems, biomechanics, bionics. E-mail: nagao@mech.ce.nihon-u.ac.jp.

in the hardness during trapezius muscle contraction are checked. Digitalization of hardness before and after shoulder stiffness treatment is conducted. Correlation between the magnitude of *BMI* and muscle hardness and judgment of hardness or softness are checked using dispersion analysis (ANOVA) and *t*-tests. The following description explains details of how the authors reached their conclusions.

2. Muscle Hardness Test Equipment

2.1 Composition of the Muscle Hardness Tester

Fig. 1 portrays the process of manual palpation (by fingers) of a muscle induration (a stiff muscle site). Human fingers are superior sensors. By pressing a finger into the skin and moving it slightly, one can readily obtain information about the induration size, hardness, and depth [18-21].

As Figs. 2 and 3 show, this proposed device can simulate the movement of a finger pushing the induration. Fig. 4 depicts the relation of the reaction force W and depth x, when the intender, representing a finger, is pushed into the skin. The intender, set in the keep plate, is put on the measured object. By holding the upper part of it by hand, the pushing is conducted at 9 mm of stroke for 5 s. The reaction force and the depth are obtained respectively from the load cell and the displacement. Then those data are sent to the PC for digital processing. With the PC, digital processing in Fig. 4 and that described hereinafter are conducted. The results are shown on the display.

The object muscle induration or muscle layers have individual differences or site differences. Consequently, because the thickness of the upper layer and the middle layer presented in Fig. 1 have individual differences and site differences, the experimenter must manipulate it by adjusting the pushing force of the finger searching for the hardness. The pushing force W_0 is equivalent to the load adjustment shown in the upper part of Fig. 2.

The main specifications are described as follows: The indenter diameter is 8 mm. Its material is POM; at the tip is a ball with 4 mm radius. The keep plate

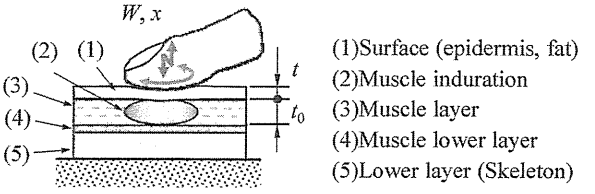

Fig. 1 Palpation of the muscle induration using a finger.

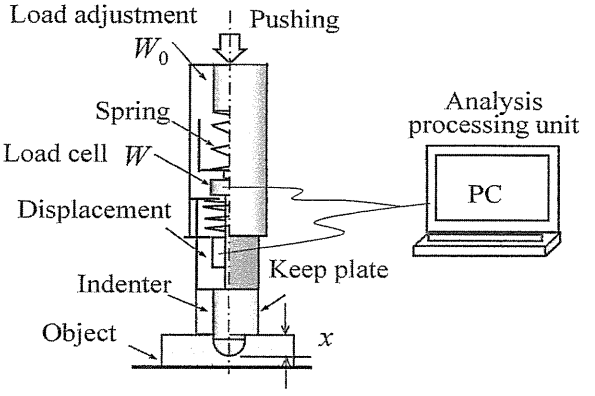

Fig. 2 Outline of the muscle hardness test equipment.

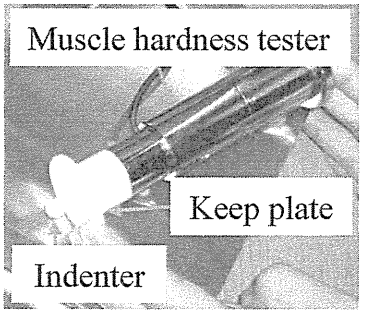

Fig. 3 Photograph showing the muscle hardness tester.

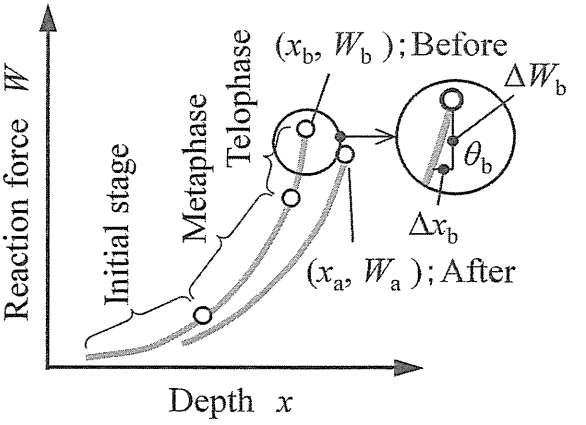

Fig. 4 Digitization of the muscle hardness (*W*-*x* curve).

diameter is 40 mm. Its material is also POM. Pushing is conducted at a stroke of 9 mm for 5 s. The range of pushing force is W_0 = 2-40 N. The range of

displacement is x = 0-15 mm. Its total height is 155 mm. Its mass is 650 g. The body casing is stainless steel (Fig. 3). It is possible to change the indenter and the keep plate depending on the figure of an object site. Additionally, W_0 is the value obtained when the tester on the steel plate 10 mm thickness is pushed into at a pushing stroke of 9 mm.

2.2 Methods of Quantification

Hardness of a stiff area or lump, as defined for this study, is the amount of resilience or repulsion that occurs when the surface part of the stiffness or lump is pushed into the surface's thickness, as presented in Fig. 1 [18-19]. This measurement is correlated with hardness sensed by palpation. Fig. 4 shows an example of W-x in which the palpated stiffness became softer after the operation than before it. The hardness is shown as that of the surface layer including the fat layer in the early period of pushing, then as the difference of hardness between the fat layer and the muscle layer, and finally as the difference of hardness between regions. To take a digital measurement of hardness, four methods are proposed as shown in Eq. (1):

$$W_b > W_a, x_b < x_a, \kappa_b > \kappa_a, \theta_b > \theta_a \quad (1)$$
$$\kappa = W/x, \tan\theta = \Delta W/\Delta x$$

With this example, let us explain Eq. (1). The pushing reaction force is described as $W_b > W_a$ (N), the pushing depth, $x_b < x_a$ (mm), the elastic constant, $\kappa = W/x$, $\kappa_b > \kappa_a$ (N/cm), and differential elastic modulus, $\tan\theta = \Delta W/\Delta x$, $\theta_b > \theta_a$ (deg). The method to describe the hardness with W or x is similar to that of the existing muscle hardness tester [2-3, 6-9], which is effective when the targeted site is restricted or for the site of which the hardness varies widely. If the method does not allow judgment of the hardness of the site, then κ is added for judgment. Even so, if it is difficult, then the difference of hardness can be quantified by adding the gradient at the end of pushing $\tan\theta$.

Alternatively, because it is possible to adjust the pushing force according to the surface thickness or the hardness of the targeted site as presented in Fig. 2, a method to obtain measurements that are approximately equal to those of the hardness felt by palpation is also possible.

3. Experiments and Results

3.1 Pushing Force Assessing the Lower Layer Hardness

We confirmed the effectiveness of our proposed digital measurement method using pushing force, which can assess the change of the lower layer hardness, by maintaining the upper layer thickness constant for two layers consisting of the upper layer of the surface layer (1) and the lower layer of the muscle layer (3) presented in Fig. 1. Conditions of the two layers are shown in Table 1.

The upper layer is made of foam rubber A ($t \times W \times \ell$ = 5 × 100 × 50 mm, E21 ± 2/5). The lower layers with different hardness are made of four kinds of foam rubber A-D ($t_0 \times W \times \ell$ = 10 × 100 × 50 mm). The combinations of composition are symbolized by AA, AB, AC, and AD. The foam rubber hardness is represented by the values of Durometer Type E. The pushing forces are divided into eight levels of 4 N to 36 N.

Results of the experiments show that the correlation between pushing reaction force W and pushing depth x are as portrayed in Fig. 5a. The elastic constant κ and the differential elastic modulus θ are in Fig. 5b. All results are mean values obtained from 10 pushing repetitions. The "4 Mono" presented in Fig. 5 means the values in directly pushing it into the samples A-D with pushing force of 4 N. To clarify the differences in measurements obtained before and after the sample, the symbols are connected with a line.

The amount of W_0 by which the differences between AA and AB, between AB and AC, and AC and AD can

Table 1 Composition of the samples[1] of two layers.

Symbol	Upper layer	Lower layer t_0 = 10 mm	Durometer Type E[2] (hardness)
AA	A-foam rubber t = 5 mm	A	E21±2/5
AB		B	E23±2/5
AC		C	E38±2/5
AD		D	E47±2/5

[1]Foam rubber dimensions: $t \times W \times \ell = t \times 50 \times 100$ mm
[2]Foam rubber hardness of from A to D

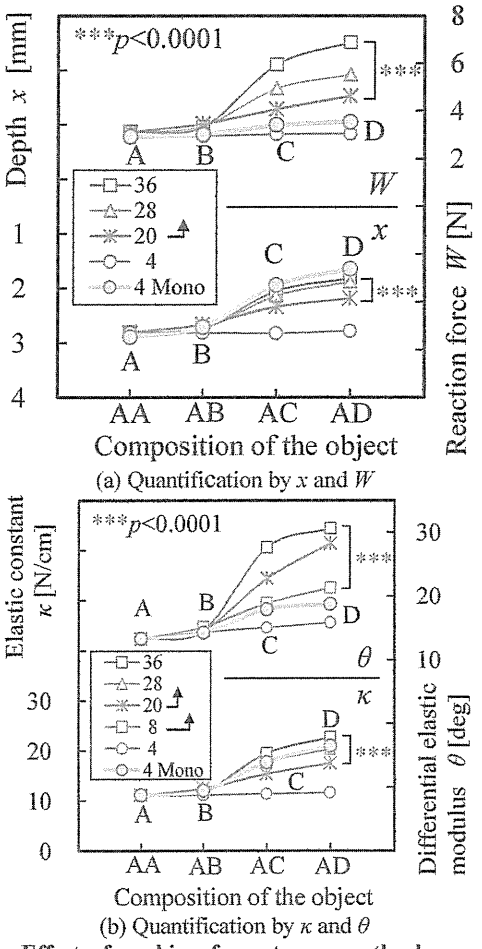

Fig. 5 Effect of pushing force to assess the lower layer hardness.

be judged, was obtained using t-tests. Assuming that the two samples are homoscedastic, the conditions were obtained with two-sided t boundary values, significance level of $p = 0.0001$, and degrees of freedom of $\varphi = 18$. The result was $t(\varphi, p) = t(18, 0.0001) = 4.97$. In terms of W_0, with the test statistic of $t_0 > t$, x, W and κ had $W_0 > 20$ N and θ had $W_0 > 8$ N. "***$p <$ 0.0001" is added to Fig. 5.

Consequently, if each pushing force equivalent to the thickness of the upper layer is appropriate, then it is possible to assess the different hardness of the lower layers digitally [18-19, 21]. It is applicable directly to the thickness of (1) and (2) in Fig. 1. In the digitalization of θ, even if W_0 is smaller than the others, the differences can be discriminated as the advantage of this equipment.

3.2 Comparison between κ and θ by the Upper Layer Thickness

We confirmed the effect of the upper layer thickness on the sensitive reference in digitalization of κ and θ when foam rubber A with thickness of $t = 1$, 2, or 3mm was put on the lower layer shown in Table 1. The results are depicted in Fig. 6. Indications "Mono" are values of A-D. In digitalization of elastic constant, as the upper layer thickens, the difference between objects becomes indistinct. Therefore, with $t = 3$ mm, it becomes more difficult to determine it than with $t = 1$ mm. However, in digitalization of θ, unlike in κ, without difference of an upper layer, we conducted an ANOVA ($p < 0.01$, one-way analysis, level of factor 4, and repetition number of times 10) for every different composition of the objects (e.g., in the case of AA, four

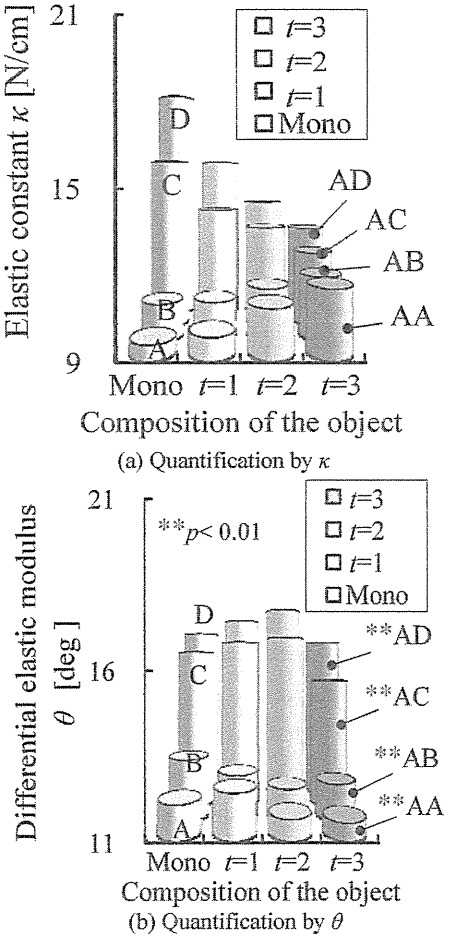

Fig. 6 Sensitivity comparison between κ and θ.

kinds of θ including single layer A, and layers with t = 1, 2, and 3 mm). The discriminant standard is that shown below.

$$F_0(\varphi_A, \varphi_E; 0.01) = F_0(3, 36; 0.01) = 4.38$$

The values F of the objects were the following: AA(1.69), AB(1.02), AC(2.64), and AD(1.57). Consequently, because $F < F_0 = 4.38$ in all the objects, it turned out to be difficult to assess the change of the upper layer thickness digitally. In Fig. 6, we described it as $^{**}p < 0.01$. In digitalization of θ, even if W_0 is small, as presented in Fig. 5, its sensitivity is so much higher than in κ to emphasize the difference of the lower layer hardness.

3.3 Contraction Hardness of Trapezius Muscle by Eversion of the Arm

This experiment confirms the possibility of digitally assessing the hardness that exists before and after a trapezius muscle contracts. The contents are shown in Tables 2-3 and Fig. 7. Examinees were six university students with different body shapes and features of physical constitution: they were designated as A1-A6 in order of increasing *BMI* (Body Mass Index) values.

The hardness of contracting muscle was obtained from the posture in which the position of upper extremity was different at two sites. First, the muscle was not tense and soft when the upper extremity was put on the armrest. Second, the muscle contracts and becomes tight when the first position of the upper extremity turns outward by 90° [22]. The site on which the intender is placed is midway between the seventh cervical spine and the acromion, where the hardness can be felt by fingers.

In Fig. 8, data for examinees A1-A6 are shown on the X axis; the hardness of the armrest position and 90-deg turning outward position in terms of κ and θ are shown on the Y axis. Along with the mean value, the range between the maximum value and the minimum value is also shown. According to $\kappa = W/x$, the difference between conditions before and after muscle contraction are evident, so it is possible to assess the muscle hardness digitally. The hardness decreases,

Table 2 Features and measurement condition of 6 examinees: university students, age 21~22.

No.	*BMI* value	Features of the body (Refer to Table 3)
A1	19	Thinness type, Thin muscle layer
A2	21	Normal type, Thick muscle layer
A3	21	Normal type
A4	22	Normal type, Tennis player
A5	24	Small fatness type
A6	24	Small fatness type, Thick muscle layer

Table 3 A position, posture, measurement condition and *BMI* value to test.

Item	Contents
Object position	Trapezius muscle of the right shoulder, the position which guesses the indenter is a midpoint of cervical spine C7 and acromial process.
Contraction action of the arm	It sits in the armchair, and positions of the arm are armchair and 90° eversion.
Measurement condition	Indentation set load W_0 = 9.8 N, keep plate diameter 40 mm, indentation setting hour 5 s, the tip is a globe on the indenter diameter at 8 mm, and pushing frequency 5 (convolution)
BMI value (kg/m^2)	Thinness type ≤ 19 19 < Normal type < 24 24 ≤ Small fatness type < 28 28 ≤ Obesity type

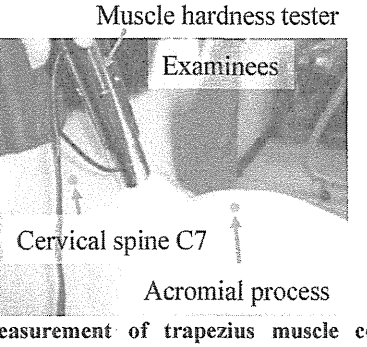

Fig. 7 Measurement of trapezius muscle contraction hardness of the right shoulder.

except for examinee A4, because the *BMI* values become greater from A1 to A6.

Although the experiment did not assess the fat layer and muscle layer thickness digitally, to assume the correlation between *BMI* and the thickness of those layers, it is reasonable to expect that the value should be smaller. Examinee A4, a tennis player, has a hard and thick neck and shoulder muscles, which are represented by the value. Examinee A6 has thick muscles. Therefore, the difference between the armrest

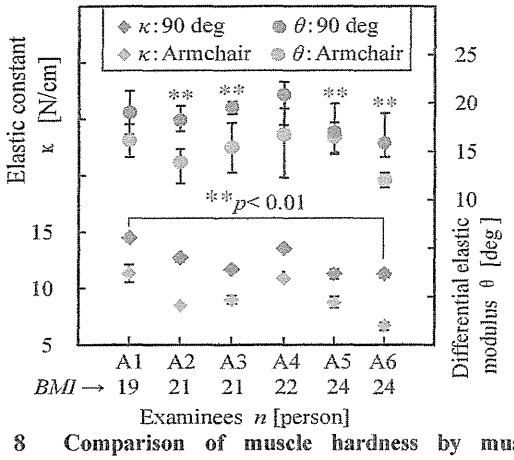

Fig. 8 Comparison of muscle hardness by muscle contraction of the trapezius muscle.

position and a 90-degree outward turning position is best. In contrast, A1, who is thin, has a large value when his upper extremity was put on the armrest. To assume that his muscle is also proportionally thin, it should be true because the value also represented the bone layer hardness as well as muscle layer or the pushing force was strong.

However, even though the tendency in digitalization by θ is like that shown by κ, results show that the variation of values is greater than that by κ. That tendency might be attributed to the high sensitivity depicted in Fig. 6. Showing the effectiveness of our proposed digitalization, when the difference in, for example, A5 is evident by κ, but it is difficult to discriminate by θ, one can discriminate it using $\kappa = W/x$.

Next, using the t-test, we confirmed that the muscle hardness in turning to an outward position can be discriminated to be higher than that in armrest position. As test conditions to ascertain the values, two samples are assumed to be homoscedastic. The t boundary value is one-way. The significance standard is $p = 0.01$. Degrees of freedom are $\varphi = 8$. In digitalization by κ and θ, $t(\varphi, 2p) = t(8, 0.01) = 2.90$ was found. In digitalization by κ, the test statistic t_0 was $t_0 > t$ in all examiners. With digitalization by θ it was so in only A2. And, with θ, A1 and A4 have no significant difference. It is shown as "$**p < 0.01$" in Fig. 8.

The experiment demonstrated the following. Fig. 1 and Table 2 show that it is important to assess the hardness of each rather than the differences of hardness among individuals because human bodies have individual differences related to the thickness and hardness of the object sites. Furthermore, as shown in Table 1 and Fig. 5, it is necessary to imitate the movement of strong pushing when the object site is thick for measurement with good sensitivity because thickness is a factor holding the key to the sensitivity of hardness. When the thickness is slight, even a small change can be grasped if one pushes the indenter lightly, as in palpation.

3.4 Muscle Hardness Related to Shoulder Stiffness

The examinees were 21 male university students aged 21-4 (B1-B21), of whom we had conducted a survey in the form of a questionnaire. We obtained their consent for the experiment in advance. The object sites were the sites of shoulder stiffness, which we located by palpation and near which the indenter was pushed, as portrayed in Fig. 7, using the same measurement conditions as those presented in Table 2. Before and after a practitioner gave an examinee a massage, we measured the hardness with our muscle hardness tester five times, with the mean considered as the measured value. The practitioner gave a massage by hand and used an ultrasonic therapy apparatus for about four minutes.

For the amount of change before and after the treatment practice, we conducted a t-test, assuming that the two samples should be homoscedastic. With a two-sided t-boundary value ($p < 0.05$), we obtained $t(\varphi, p) = t(8, 0.05) = 2.31$. The examinees were divided into three groups based on this test: a group of the examinees of whom muscles softened (13 by κ and 9 by θ among 21), a group showing no difference (5 by κ and 11 by θ among 21), and a group of examinees whose muscles became harder (3 by κ and 1 by θ among 21).

In Fig. 9, with κ represented on the left vertical axis, the three groups are shown from right to left (represented by two bar charts). They are arranged in ascending order of muscle hardness. The horizontal axis represents the values of examinee numbers and

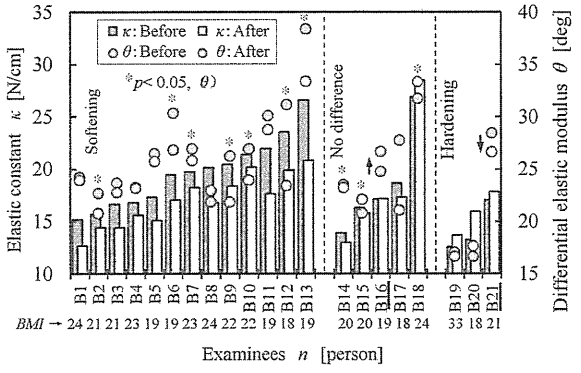

Fig. 9 Muscle hardness of shoulder stiffness.

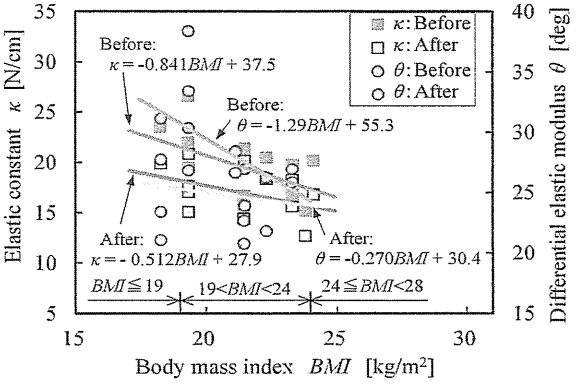

Fig. 10 Correlation of muscle hardness and *BMI*.

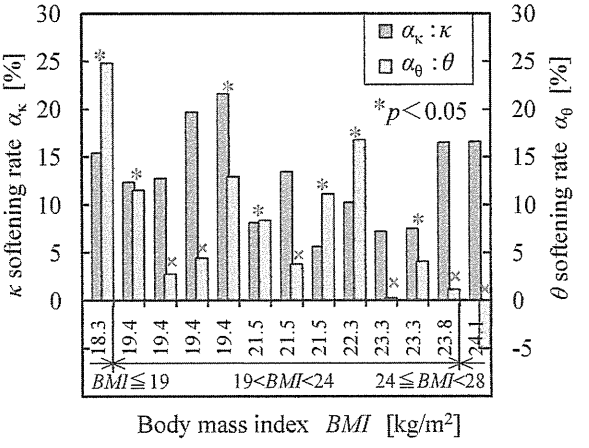

Fig. 11 Relation between *BMI* and muscle hardness softening rate.

their *BMI*. On the other hand, with θ represented on the right vertical axis (by signs of circle), each θ of the examinees, divided into three groups by *t*-test, is marked using a reference mark [*] (*$p < 0.05$).

They were divided into three groups because the practitioner explains that physical stimulus was given to a stiff muscle for which the tissues' blood circulation was facilitated, thereby softening it. Others showed no difference. Other muscles showed increasing inner pressure of the muscle, thereby hardening it. B16 (no difference by κ, hardening by θ; ↑) and B21 (hardening by κ, softening by θ; ↓) showed different judgment by κ and θ. With the boundary value of $p < 0.01$, they have the same judgment by κ and θ. Therefore, it is possible to assess the muscle hardness digitally based on changes that occur during physical treatment for patients with complaints of shoulder stiffness. Results show the capability of digital assessment of the effects of practical treatment and palpation.

Next, targeting the group of examinees whose muscle was softened (among 21, with κ, 13; with θ, 9), Fig. 10 shows *BMI* on the horizontal axis in increasing order, with a regression line. After operation, the amount of softening was likely to be greater because the *BMI* was smaller in a lean body frame. In contrast, the softening was likely to be smaller in an obese body frame, with a downward-sloping regression line. The thickness presented in Fig. 1 might be correlated to the amount of *BMI*. Fig. 10 shows that, as *BMI* decreases, the procedure is more likely to have the effect of softening on it.

Defining the levels of softening digitalized by κ and θ as the softening rate, they were gained by Eq. (2), as presented in Fig. 11. The examinees were 13, whose muscles were softened with κ, and to which θ was also accorded. Suffix a and suffix b respectively denote values obtained after operation and before operation. Furthermore, α_κ and α_θ respectively represent the elastic constant and softening rate by the differential elastic modulus.

$$\alpha_\kappa = 1 - \frac{\kappa_a}{\kappa_b}, \quad \alpha_\theta = 1 - \frac{\theta_a}{\theta_b} \tag{2}$$

The horizontal axis shows the order of *BMI* values. The vertical axis shows the softening rate, α_κ and α_θ. The bar charts show digitalized levels of softening. With this extent of *BMI*, the level of softening does not depend on the amount of *BMI*. In other words, because the levels of softening had individual differences even with the same procedure, it is necessary to conduct

procedures suited for each condition of stiffness. The sign "*" in the figures like Fig. 9, shows a significant difference between κ and θ. Sign "×" denotes a lack of significant difference. The formula is helpful to objectify the results of procedures because it can digitalize the results of softening by procedure.

4. Conclusions

Proposing an outline of the muscle hardness tester that can imitate hardness assessments done by palpation and presenting a mode of to digital assessment, we were able to confirm their effectiveness and validity by conducting several experiments. The obtained results are summarized as follows:

- We proposed four methods to assess muscle hardness digitally. Using them singly or multiply, the tester presents high reliability. κ and θ are used in typical methods;
- It is suggested that the levels of softening before and after operation should be able to be digitalized by softening ratio, which can also be useful to objectify the effectiveness of operation;
- Discriminating the lower layer hardness for different surface thickness is possible if the pushing force is appropriate to thickness;
- For a thin surface layer, such as a few millimeters, θ has less effect on the lower layer hardness than κ does, and is therefore validated. Furthermore, θ is more sensitive than κ;
- When a difference between hardening and softening is visible as in the contracted and stiff trapezius muscle of a shoulder, digital assessment by W, x, or κ is sufficient. Even if the object sites are the same, they have individual differences reflected in the values, which suggests the need for measurement conditions and data management tailored to respective examinees;
- The muscle hardness before and after practical treatment for shoulder stiffness are categorizable into three groups: softening, no difference, or hardening. They are highly correlated to κ and θ, with some exceptions;
- As *BMI* becomes larger, the hardness value becomes smaller. That tendency suggests that the surface layer thickness can be expected to correlate to the *BMI* amount;
- In future studies, we will aim at improving the process for practical application by examining the possibilities of digitally assessing effects according to practices, substitution of palpation or self-palpation, and follow-up.

Acknowledgments

Part of this study is conducted with assistance provided by a Grant-in-Aid for Scientific Research C (No. 22560225) of the Japan Society for the Promotion of Science. We express our gratitude for that support.

References

[1] M. Nagao, O. Yokota, Hardness test method, hardness test equipment and hardness measuring device, Nihon Univ., Patent No. 5046207 JP, 2012.
[2] Imoto machinery Co. Ltd., The muscle hardness tester, Patent No.3951257 JP, 2007.
[3] S. Hiwatari, Y. Nagahama, The muscle hardness tester, Patent No.4352022 JP, 2009.
[4] Y. Arima, Objectification of hardness information of palpation, Bulletin of Meiji University of Oriental Medicine 25 (1997) 25-49.
[5] F. Ito, K. Oosaki, K. Takahashi, H. Hara, The effects of electric field therapeutic device (Healthtron) on the stiffness in the neck and shoulder area, J. Jpn. Soc. Balneol. Climatol. Phys. Med. 68 (2) (2005) 110-121.
[6] H. Andersen, L.A. Nielsen, B.D. Samsoe, T.G. Nielsen, Pressure pain sensitivity and hardness along human normal and sensitized muscle, Somatosensory and Motor Research 23 (3) (2006) 97-109.
[7] M. Ashina, L. Bendtsen, R. Jensen, F. Sakai, J. Olesen, Measurement of muscle hardness: A methodological study, Cephalalgia Technical Note 18 (1998) 106-111.
[8] Ito Co. Ltd., The muscular tissue hardness tester, Patent No.4922056 JP, 2012.
[9] A. Takanashi, H. Karasuno, M. Katou, R. Konuma, K. Shiota, T. Matsuda, et al., Reliability of measurement of elastomer samples by soft tissue stiffness meter, Rigakuryoho Kagaku 24 (1) (2009) 31-34.
[10] T. Uchiyama, K. Ohsugi, M. Murayama, Evaluation of muscle hardness by indentation method, Biomechanisms 18 (2006) 219-227.
[11] N. Motooka, S. Omata, J. Koizumi, K. Yamaguchi,

Development of new instrument to assess visco-elasticity of skin and muscle, in: Technical Digest of the 15th Sensor Symp., 1992, Kawasaki, Japan, pp. 87-92.

[12] Y. Karugome, Hakuju Co. Ltd., Hardness measurement of muscle and muscle hardness measuring device, Patent No.2008-168063 JP, 2008.

[13] T. Irie, H. Oka, Measurement of biomechanical properties by impact response (II), Biomechanisms 24 (3) (2000) 168-173.

[14] Y. Tsuda, S. Uchida, I. Kumamoto, H. Sugano, K. Nitta, An examination for measuring the softness of human shoulders (1), J. Intl. Soc. Life Info. Sci. 23 (2) (2005) 332-334.

[15] K. Kamiyama, N. Kawata, M. Mizuma, Changes of muscle hardness of per and post physical exercise of the extensor carpi radialis longus, Showa Univ. J. Med. Sci. 24 (3) (2004) 494-498.

[16] T. Irie, H. Oka, Effect of rest time on isometric muscle fatigue measured by biomechanical impedance, Trans. Jpn. Soc. Mech. Eng. A 71 (703) (2005) 507-512.

[17] K. Ohta, T. Yano, Comparison study between superficial and deep acupuncture on the neck and shoulder stiffness, J. Jpn. Soc. Balneol. Climatol. Phys. Med. 68 (2) (2005) 122-133.

[18] M. Nagao, Y. Sakai, O. Yokota, Development of non-contact softness tester, J. Jpn. Soc. Design Eng. 41 (5) (2006) 267-272.

[19] M. Nagao, O. Yokota, Development of softness testing equipment using balloon, J. Jpn. Soc. Design Eng. 41 (11) (2006) 583-588.

[20] R. Umeda, M. Nagao, O. Yokota, A proposal a contactless measurement method that considers the viscoelasticity, in: 24th ISPE International Conference on CAD/CAM, Robotics and Factories of the Future, July 29-31, 2008, Koriyama, Japan.

[21] M. Nagao, O. Yokota, M. Yoda, Development of functional testing equipment measured softness, Trans. Jpn. Soc. Mech. Eng. C 76 (770) (2010) 2598-2603.

[22] M. Murayama, K. Nosaka, T. Yoneda, K. Minamitani, Changes in hardness of the human elbow flexor muscles after eccentric exercise, Eur. J. Appl. Physiol. 82 (2000) 361-367.

講演

人工の擬似しこりを用いた筋硬度計の硬軟探索に関する研究*

Study on Hard and Soft Search with Muscle Hardness Tester Using Artificial Para-Stiffness

長尾　光雄*1 (Mitsuo NAGAO)　遠藤　徳雄*2 (Tokuo ENDO)　横田　理*1 (Osamu YOKOTA)　紺野　愼一*3 (Shin-ichi KONNO)

1. 緒　論

肩こりや腰痛は国民的な健康を害する症状の一つであり，発症部位にはしこりやこわばりによる痛みなどの自覚症状が伴う．肩こりは症状名であり整形外科的疾患の中では狭義の頚肩腕症候群に分類され，しこりは筋硬結と呼ばれる．しこりの位置や形状および硬軟または押し返しの形態には個体差がある．施術する柔道整復師(以降では験者と呼ぶ)は，患者さん(以降では被験者と呼ぶ)に対して触診や問診により多くの情報を得ることができる．これにより施行内容や因果関係などを推定し，施行や生活指導にあたっている．指先や手のひらで触診するときには，患部に対して押し圧を変えながら摩(さす)る行為により情報を得ている．これら一連の動作を探索と呼ぶことにする．しこりの硬軟を判別する際には，脂肪層を含んだ表層（または表皮組織，あるいは軟部皮下組織）や筋肉層の厚薄度合により，指の押し圧を調整している．ここで，しこりの硬軟について定義すれば，金属材料の硬軟とは意味が異なり，柔軟物の弾力の強さ度合を硬軟の意味として用いる．

このような背景において，硬軟を数値化するために押し圧の加減を模倣した筋硬度計[1), 2)]の開発を進めている．目的は，押し込む加減でしこりの硬軟が検知可能であるのか確認することにある．

この方法には，スポンジゴムにより組み合せた人工の擬似モデルを提案し，これらの条件に適った押し加減について検証実験を行った．その結果からは，擬似表層の厚薄に適った加減の必要性が分かった．以下に，これらの結論に至った内容を述べる．

*　原稿受付　2012年9月28日
*1　正会員，日本大学
*2　非会員，遠藤整骨院
*3　非会員，福島県立医科大学

2. 擬似モデル

2.1 硬軟の数値化

図1は指により表層を介してしこりを探索する様子について模型的に表したものである．図2はこの指を模倣した圧子を備えた筋硬度計[1)]であり，対象物からの押込み反力Wと対象物への押込み深さxが測定できるため，図3のW-x線図が得られる．しこりの硬さがA>Bにおいて，例えば，押込み設定荷

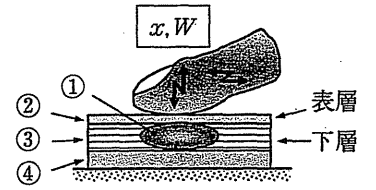

①筋硬結(しこり) /擬似しこり /U_0(A-D)
②表層(表皮, 脂肪) /擬似表層 /U_1-U_4
③筋肉層,　④骨格層 /測定盤

図1　しこり探索の説明と擬似モデル

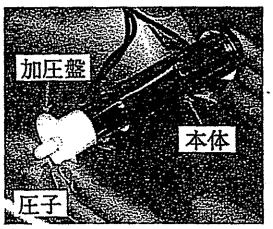

図2　筋硬度計測装置の測定部

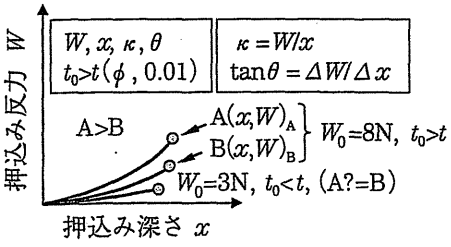

図3　しこりの硬軟「A>B」のW-x線図

表1　提案する擬似モデルの分類と生体との相関一覧

	(1)	(2)	(3)	(4)	備　考
BMI[kg/m^2]	$BMI<19$	$19\leqq BMI\leqq 24$	$24<BMI\leqq 28$	$28<BMI$	左記項目の関連性には個体差があり，必ずしもBMI値と相関しない事例もある．
体　型	痩せ型	普通（標準）型	小太り型	肥満型	
表層の厚さ（上層）	薄い(a)	普通(b)	少し厚い(c)	厚い(d)	
	$a<b<c<d$				
筋肉層の厚さ（下層）	薄い(α)	普通(β)	少し厚い(γ)	厚い(δ)	
	$\alpha<\beta<\gamma<\delta$				
触診押込み強さ W_f[N]	軽い(W_a)	普通(W_b)	少し強い(W_c)	強い(W_d)	
	$W_a<W_b<W_c<W_d$				
擬似表層	U_1	U_2	U_3	U_4	(上層)
擬似しこり	U_0(A, B, C, D), 硬軟 A>B>C>D				(下層)
W_0[N]	3～5	3～8	3～10	3～13	押込み設定荷重

重W_0=3Nの際にはAとBの判別はできないが，W_0=8NではA>Bの判別ができる例である．

硬軟の数値化は，W-x線図に示す終端の押込み深さxや押込み反力W，および弾性定数κや微分弾性定数$\tan\theta$で行ない，硬軟の違いはこれらを総合して判別することも提案している．

2.2　擬似しこり

図1は指でしこりを探索するときの動作を説明したものであり，臨床では矢印で示した動きから，しこりの情報(x, W)を得ながら直ちに施術に移行する場合が多い．実験の擬似モデルの構成は，図のように擬似しこりの層を擬似表層と測定盤で挟み込んだ3層になっている．

表1には提案する擬似しこりの分類と生体との相関に係わる一覧を示す．分類は(1)から(4)に分けてあり，その根拠は体型の分類にある．その体型には，表層の厚薄により分類しており，BMI値と相関が高いとの考えから，表のBMIの範囲で4段階に分類した．筋肉層の厚薄もこれと相関するものと考えているため，しこりを触診する押込み強さもこれと相応するものとした．すなわち，図1に示す擬似モデルに相当させた表中の擬似表層U_1からU_4とおき，擬似しこりもU_0(A, B, CおよびD)の4種類とした．表2は擬似表層，表3は擬似しこりに用いたスポンジゴムを示す．

これらの組み合わせは臨床の験者からの提案によるものであるが，験者が経験した最大最小とその中間としたもので，すべての被験者を対象としたものではなく，その代表的な事例について取り上げたものであることを断っておく．

表2　擬似表層の材料

種　類	記号(厚さmm)	硬　度
パ　フ	U_1(t2)	20±1.0[1]
	U_2(t4)	
CRゴム/軟質	U_3(t3)	25±0.5[2]
CRゴム/最軟質	U_4(t5)	16±0.5[2]

1) FP型デュロメータ，FP硬度，測定した試料の寸法 $t\times W\times D$=8×54×54[mm]
2) E型デュロメータ，E硬度，測定した試料の寸法 $t\times W\times D$=10×100×50[mm]

表3　擬似しこりの材料

種　類	記号,U_0	硬　度[2]
CRゴム/硬質	A	49±1.0
シリコーンゴム	B	42±0.5
CRゴム/軟質	C	28±1.5
CRゴム/最軟質	D	16±0.5

3.　実　験

3.1　押込み圧の加減

擬似表層の厚薄に適応した圧子からの押込み圧の加減は，図2の本体上部に設けた調整部により行なう構成になっており，実験ではこれを押込み設定荷重W_0と表す．表1に示す擬似表層に対応した押込み設定荷重は下段に示した．最小値W_0=3Nとした理由は，4種類の擬似しこりを組み合わせたAB，BCおよびCDにおいて，その平均値の差をt検定($p<0.01$)により有意に差が認められたときのW_0の値である(図3参照)．U_1からU_4では，この結果からW_0=3Nを基準として段階的に与えて，有意差が検定できた時点で終了とした．

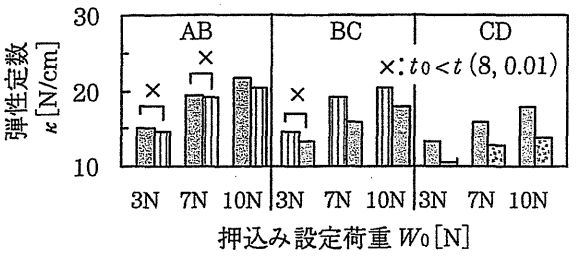

図4　擬似表層 U_3 の擬似モデルの弾性定数

ここで比較対象としたAB，BCおよびCDの組合せとした理由は，各組の前に示したA，BおよびCは施術前のしこりの状態をモデル化し，これに対して後に示したB，CおよびDは施術後にそれぞれ軟化した状態を想定したものである．

3.2　筋硬度計測装置の条件

図2に示す本体からの W と x のデータはノートPCに取り込まれて図3が得られる．このデータから W，x，κ および θ を求める．圧子の寸法は直径8mmで先端が半球面であり，押込みストロークは9mm一定，押込み動作時間は5秒以内，押込み設定荷重は上部のばねと調整部で設定する．検定処理対象データは5回とした．

4.　結果と考察

4.1　押込み圧の加減

図4は擬似モデル(3)の U_3 に対して押込み設定荷重を強くしたことで，擬似しこり3組の有意差が認められる W_0 の経過を示した代表例である．これは弾性定数において，等分散を仮定した2標本による平均値の差を t 検定(p<0.01)したもので，t_0(検定統計量)と t(両側境界値)による有意差を判定した場合である．

擬似しこり3組のAB，BCとCDの検定の結果は，組み合わせABの押込み設定荷重 W_0 が3Nと7Nではその差(t_0<t；図中×印)の違いは認められないがこれを10Nとした場合にはその差(t_0>t)の違いが認められた．BCの組み合わせでも7N以上から認められている．このように，擬似表層を介して擬似しこりの硬軟の違いを数値化するためには，擬似表層の厚薄や硬軟の影響も受けるので，これらの条件に適った押込み圧を加減する必要がある．硬軟を検知する押込み圧が与えられなかった場合や押込み圧が強すぎた場合には，その差の判別はできないことも示唆している．

4.2　擬似しこりの硬軟

表4には表1の擬似モデル(1)から(4)および U_0 の結果を表した．U_1 から U_4 に示す押込み設定荷重 W_0 は，基準の3Nと4N，8N，10Nおよび13Nの検定結果を示す．これも表中の○印は，組み合わせの有意差 t_0>t=t(8, 0.01)が認められた場合，×印はその差の違いが認められなかった場合である．初期の3Nの条件では，U_0(4種類の擬似しこり単体)はすべての組合せにおいて，差の違いが認められる．これに対して，U_1 から U_4 のように擬似表層が厚くまたは硬さが増すとその差の違いが認められなくなり，W と x はその傾向が顕著である．この W に関して表したものが図5である．U_3 と U_4 ではすべての組み合わせで差の判別ができていない．これに対し

表4　擬似モデルと押込み設定荷重の実験結果（t検定）

評価	擬似しこりの組み合わせ	擬似しこりと擬似表層の条件および押込み設定荷重 W_0								
		U_0	U_1		U_2		U_3		U_4	
		3N	3N	4N	3N	8N	3N	10N	3N	13N
押込み反力 W [N]	AB	○	×	○	×	○	×	×	×	○
	BC	○	○	○	○	○	×	○	×	×
	CD	○	○	○	○	○	×	○	×	○
押込み深さ x [mm]	AB	○	×	○	×	○	×	○	×	○
	BC	○	○	○	○	○	×	○	×	○
	CD	○	○	○	○	○	○	○	○	○
弾性定数 κ [N/cm]	AB	○	○	○	×	○	×	○	×	○
	BC	○	○	○	○	○	×	○	×	○
	CD	○	○	○	○	○	○	○	○	○
微分弾性定数 θ [deg]	AB	○	○	○	○	○	×	○	×	○
	BC	○	○	○	○	○	○	○	○	○
	CD	○	○	○	○	○	○	○	○	○